

# Zeolite-NaY-supported Ir/Sn catalysts derived from single- and dual-source organometallic precursors. Preparation and characterization of highly selective dehydrogenation catalysts

David M. Somerville and John R. Shapley \*

*Department of Chemistry, University of Illinois at Urbana-Champaign, Urbana, IL 61801, USA*

Received 13 January 1998; accepted 8 April 1998

Zeolite-NaY-supported Ir/Sn catalysts (1 wt% Ir, 0.6 wt% Sn; 1 : 1 molar ratio) were prepared by adsorption of the organometallic precursors  $\text{Ir}(\text{CO})_2(\text{acac})$  and  $\text{SnMe}_3\text{OH}$  or  $(\text{COD})_2\text{Ir-SnMe}_3$  ( $\text{COD} = 1,5\text{-cyclooctadiene}$ ) from hexane solutions followed by activation in  $\text{H}_2$  up to 773 K. The Ir/Sn/NaY catalysts displayed high selectivity for the dehydrogenation of propane to propene at ca. 773 K and, in the presence of  $\text{H}_2$ , maintained thermodynamic conversion levels for up to 24 h. After activation, the catalyst derived from the dual-source precursors (Ir + Sn/NaY) appeared homogeneous in composition, whereas the catalyst derived from the single-source precursor (Ir-Sn/NaY) appeared heterogeneous with distinct regions of visible particles. Scanning transmission electron microscopy revealed that the nanoscale metal particles present were small and uniform in size (ca. 1 nm) in the Ir + Sn/NaY catalyst but ranged in size from 1 to 10 nm in the Ir-Sn/NaY catalyst. Energy-dispersive X-ray analysis showed that bimetallic particles were formed for both catalysts. Temperature-programmed reaction of chemisorbed carbon monoxide indicated that the Ir/Sn/NaY catalysts were electronically modified by the presence of tin in comparison with analogously prepared Ir/NaY catalysts.

**Keywords:** iridium, tin, NaY, alkane dehydrogenation

## 1. Introduction

Heterogeneous catalyst systems composed of more than one metal component are of paramount importance in modern catalysis [1]. Multicomponent catalysts have found widespread use, as the combination of two or more metals can lead to synergistic effects such as increased activity, enhanced catalyst lifetime, and improved product selectivity. The changes in catalytic behavior that occur upon adding an inert element to a noble metal have been well documented [2,3]. The changes in catalytic activity are attributed to a decrease in the number of contiguous active sites (ensemble effect) as well as to changes in the electronic nature of the active metal particles (ligand effect) [4]. The relative importance of “ensemble” and “ligand” effects is exceedingly difficult to determine, especially as adequate probes for ligand effects are often lacking.

Although an extraordinarily large number of bimetallic catalysts has been examined by various researchers, a brief survey of recent literature demonstrates the great interest in the Pt/Sn catalyst system [5–14]. Multicomponent catalysts based upon the Pt/Sn combination have found widespread industrial usage, and recent patents involving the Pt/Sn system include catalysts for naphtha reforming [15,16], reduction of nitrogen oxides in flue gases [17], and the dehydrogenation of light alkanes [18]. Other Pt/Sn systems of interest include Pt/Ir/Sn catalysts, which have found use for naphtha reforming [19], alkane dehydrogenation [20], and the purification of automobile exhaust [21]. Given

the large amount of interest in the Pt/Sn catalyst system, it is surprising to find that very little work has been performed on the closely related system, Ir/Sn. Examination of the Ir/Sn system is attractive, as previous authors have noted [22,23], since it provides an interesting prospect for comparison with the Pt/Sn and may also have significant catalytic properties of its own. Examination of the Ir/Sn system could also shed light on the role of Ir in Pt/Ir/Sn catalyst systems [19–21].

Previous studies of the Ir/Sn system by other researchers have utilized high metal loadings (10 wt%, Ir + Sn) supported on  $\text{Al}_2\text{O}_3$  and  $\text{SiO}_2$  [22,23]. The  $\text{Al}_2\text{O}_3$ -supported Ir/Sn catalyst was extremely selective for the dehydrogenation of cyclohexane to benzene and also displayed considerable activity for benzene hydrogenation at room temperature. In contrast, the  $\text{SiO}_2$ -supported Ir/Sn system displayed low activity for benzene hydrogenation when the catalyst was reduced at low temperatures, and displayed no activity when reduced at high temperatures. The lack of activity for the  $\text{SiO}_2$ -supported catalysts was attributed to the formation of catalytically inactive Ir/Sn alloys, whereas the activity of the  $\text{Al}_2\text{O}_3$ -supported catalysts was attributed to the presence of free Ir particles [23].

In view of the differences between  $\text{Al}_2\text{O}_3$ - and  $\text{SiO}_2$ -supported Ir/Sn catalysts, we thought it would be of interest to explore the activity of this combination on a related important catalyst support material, namely zeolite NaY. Our work also provides a comparison with recent studies on the related Pt/Sn/NaY system [24]. In this study, we have examined the preparation of Ir/Sn/NaY catalysts from

\* To whom correspondence should be addressed.

both single-source and dual-source organometallic precursors.

## 2. Experimental

**Catalyst preparation:** The organometallic compounds  $(\text{COD})_2\text{Ir-SnMe}_3$  [25] and  $\text{Ir}(\text{CO})_2(\text{acac})$  [26] were prepared according to literature procedures;  $\text{Sn}(\text{Me})_3\text{OH}$  was used as received (Strem). Zeolite NaY (LZ-Y52, Union Carbide) was treated under vacuum at 423 K for ca. two hours prior to use.

Three catalysts, each nominally 1 wt% Ir, were prepared by adsorption of organometallic precursors into zeolite NaY from hexane solutions. The first catalyst, Ir/NaY, was prepared from  $\text{Ir}(\text{CO})_2(\text{acac})$  (37 mg) in hexane (25 ml) with NaY (2 g). The slurry was stirred under  $\text{N}_2$  for 12–16 h to ensure complete adsorption. The solvent was then removed under vacuum, and the resulting solid material stored under  $\text{N}_2$  until use. The second catalyst, Ir + Sn/NaY, was prepared in an analogous manner by adsorption of  $\text{Ir}(\text{CO})_2(\text{acac})$  (37 mg) and  $\text{SnMe}_3\text{OH}$  (18 mg) to produce a material with the nominal composition of 1 wt% Ir and 0.6 wt% Sn, which is a 1:1 molar ratio of Ir to Sn. The third catalyst, Ir-Sn/NaY, was prepared in an analogous manner by adsorption of  $(\text{COD})_2\text{Ir-SnMe}_3$  (60 mg) to produce a catalyst with the same nominal composition as Ir + Sn/NaY.

**Propane dehydrogenation and hydrogenolysis:** The zeolite-supported catalyst samples (ca. 250 mg) were activated and tested on a catalyst line that includes a gas-handling system, catalytic reactor, and equipment for analysis of the effluent [27]. Streams of hydrogen (Matheson, 99.999%), propane (Matheson, 99.5%), and He (Matheson, 99.995%) were deoxygenated over  $\text{Cr}(\text{II})/\text{SiO}_2$  and dried over activated molecular sieves. The catalysts were placed in a Pyrex U-tube reactor containing a coarse frit supporting the catalyst bed, which was in contact with a thermocouple well containing an Omega type k chromel/alumel thermocouple. The reactor was heated by a tube furnace controlled with an Omega CN2011 temperature controller. A Packard model 430 gas chromatograph with a flame-ionization detector was used to separate and quantify the hydrocarbon products ( $1/8'' \times 7'$ , 10 wt% *n*-octane/Porasil column). The effluent was also monitored by a computer-interfaced Dyco quadrupole mass spectrometer (model M100M), which was connected immediately downstream from the reactor by a silica capillary.

Prior to activation, each sample was flushed with  $\text{H}_2$  for 15–30 min to displace any air introduced into the system while loading the catalyst. The samples were activated by heating to 773 K (at 15 K/min) under a stream of  $\text{H}_2$  (40 ml/min) and holding at 773 K for one hour. The samples were taken to the desired temperature under a continuous stream of  $\text{H}_2$ , and the appropriate reactant gas stream was introduced to the catalyst. A hydrogen-rich gas mixture ( $\text{H}_2 : \text{C}_3\text{H}_8 = 40 : 4$  ml/min) was used for hydrogenolysis studies, while dehydrogenation studies were conducted

with a gas mixture containing He,  $\text{H}_2$ , and  $\text{C}_3\text{H}_8$  in a ratio of either 40 : 5 : 5 or 40 : 0 : 5 ml/min.

**STEM and EDX:** Electron microscopy and energy-dispersive X-ray (EDX) analysis were performed with a Vacuum Generators HB501 STEM operating at 100 kV. Catalyst samples were examined after hydrogenolysis experiments and were prepared by application of a drop of catalyst material (dispersed by sonification of the catalyst in a methanol bath) onto a holey carbon grid (SPI Supplies). EDX data acquisition and analysis was performed with Link ISIS software.

**Temperature-programmed reaction (TPRE) of carbon monoxide:** The following procedure was adopted for this reaction probe. A freshly activated catalyst (400 mg) was cooled to 298 K in a  $\text{H}_2$  flow and was then exposed to CO at 298 K for two hours. The sample was first evacuated for 30 min and then flushed with  $\text{H}_2$  for another 15 min to remove any free CO. The catalyst was then subjected to a  $\text{H}_2$  flow (40 ml/min) and heated to 773 K at a rate of 20 K/min, while the effluent was monitored by mass spectroscopy.

**Ir/NaY:** The Ir/NaY catalyst system has been characterized in detail by STEM, EXAFS, XANES, and FTIR [28]. The Ir particles in this catalyst system can best be described as ca. 4–6 Ir atom clusters encapsulated within the zeolite matrix of NaY.

## 3. Results

**Catalyst preparation:** Adsorption of  $\text{Ir}(\text{CO})_2(\text{acac})$  and  $\text{SnMe}_3\text{OH}$  by the zeolite resulted in the zeolite becoming yellow and the previously yellow hexane solution becoming colorless. Activation of this zeolite sample in  $\text{H}_2$  at 773 K resulted in a light gray material (Ir + Sn/NaY) that appeared homogeneous in composition.

Absorption of  $(\text{COD})_2\text{Ir-SnMe}_3$  immediately caused the zeolite to turn light red, and the previously yellow hexane solution became colorless. Removal of the solvent from the zeolite impregnated with  $(\text{COD})_2\text{Ir-SnMe}_3$  produced a material that had an obvious sharp odor. A sample of the freshly impregnated zeolite was loaded into a crucible, and the electron impact mass spectrum was recorded for the volatile components. This indicated that the volatile species generated  $\text{C}_7/\text{C}_8$  fragments as well as those due to hexane, apparently remaining from the impregnation step. Activation of the zeolite impregnated with  $(\text{COD})_2\text{Ir-SnMe}_3$  in  $\text{H}_2$  at 773 K resulted in the formation of a light gray material (Ir-Sn/NaY) that was visibly speckled with light green spots ca. 0.5 mm in diameter. Examination of both of these activated Ir/Sn/NaY materials by powder XRD showed no diffraction lines that could be distinguished from the NaY background.

**Electron microscopy/energy-dispersive X-ray analysis:** Electron micrographs of the Ir + Sn/NaY material indicated that the metal particles in this system were evenly dispersed and were in the 1 nm size range. The electron micrographs obtained for the Ir-Sn/NaY material showed

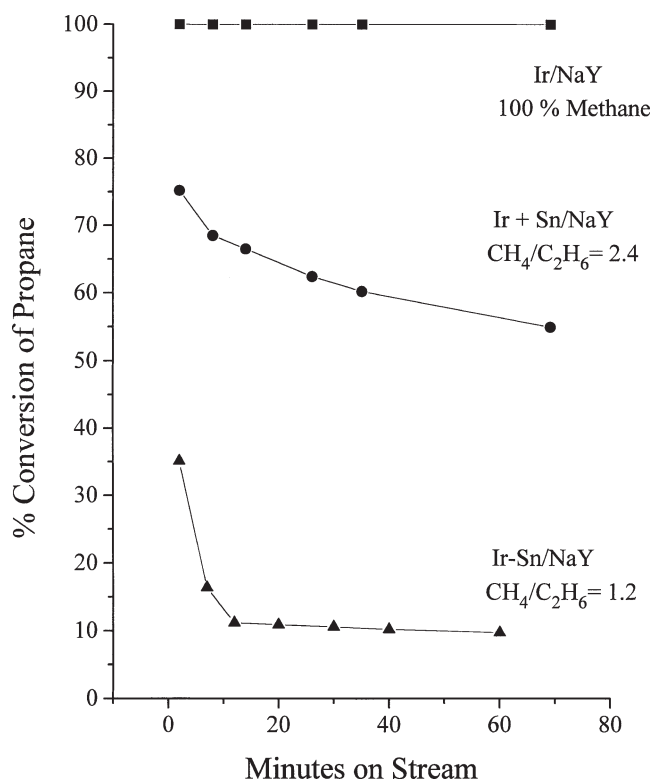


Figure 1. Propane hydrogenolysis. Reaction conditions: 773 K,  $\text{H}_2$ :  $\text{C}_3\text{H}_8 = 40:4$  ml/min. (■) Ir/NaY, (●) Ir + Sn/NaY, (▲) Ir-Sn/NaY.

that the nanoscale metal particles present in this system were unevenly distributed and ranged in size from 1 to 10 nm.

EDX analysis established that bimetallic particles were formed in both Ir/Sn/NaY catalysts. The growth of the smaller particles under the influence of the electron stream and the overlap of the Cu  $L_{III}$  line (from the holey carbon grid) with the Ir  $L_{III}M_I$  line (8.047 and 8.045 keV, respectively) hampered the quantitative determination of particle composition. Qualitatively, it was found that the larger metal particles (>5 nm) of Ir-Sn/NaY were approximately 1:1 Ir/Sn alloys, while the smaller particles (1 nm) present in Ir + Sn/NaY appeared to be Ir-rich (Ir/Sn  $\approx$  1.3–4.0). EDX analysis of featureless areas of the catalysts showed the presence of Sn but not Ir.

**Propane hydrogenolysis:** The results from the hydrogenolysis of propane, examined at 773 K, are given in figure 1. Shown for comparison is the Ir/NaY catalyst, which was highly active and produced 100% methane under these reaction conditions ( $\text{H}_2$ : $\text{C}_3\text{H}_8 = 40:4$  ml/min). Both Ir/Sn/NaY catalysts had lower primary hydrogenolysis activities, as shown by the lower total conversion of propane to methane and ethane, as well as a decreased amount of secondary hydrogenolysis, as indicated by the low  $\text{CH}_4/\text{C}_2\text{H}_6$  ratios. However, the Ir/Sn catalyst derived from a single-source precursor, Ir-Sn/NaY, had a significantly lower overall hydrogenolysis activity, in both primary and secondary reactions, than the catalyst derived from dual precursors, Ir + Sn/NaY.

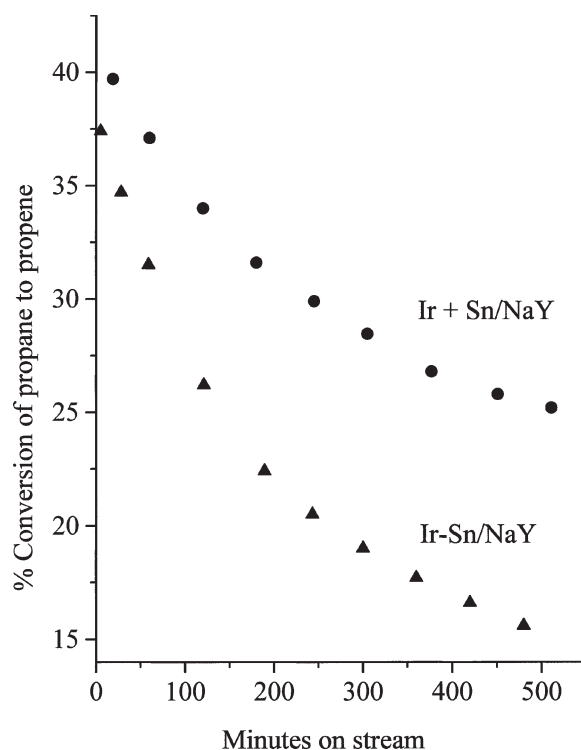


Figure 2. Propane dehydrogenation. Reaction conditions: 773 K, He:  $\text{C}_3\text{H}_8 = 40:5$  ml/min. (●) Ir + Sn/NaY, (▲) Ir-Sn/NaY.

**Propane dehydrogenation:** Propane dehydrogenation was conducted both in the presence and absence of excess  $\text{H}_2$ . In the absence of excess  $\text{H}_2$  (He: $\text{C}_3\text{H}_8 = 40:5$  ml/min, 773 K), both Ir/Sn catalysts were highly selective for the production of propene (95–98%), but underwent substantial deactivation with time on stream (figure 2). In the presence of excess  $\text{H}_2$  (He: $\text{H}_2$ : $\text{C}_3\text{H}_8 = 40:5:5$  ml/min, 773 K) both Ir/Sn catalysts maintained high selectivity towards propene, but were much more stable with time. The catalytic behavior of the Ir/Sn catalysts is shown in figure 3 and compared to Ir/NaY. No deactivation of the Ir/Sn catalysts was observed during dehydrogenation experiments conducted in the presence of  $\text{H}_2$ . Specifically, for Ir + Sn/NaY, the activity and selectivity displayed in figure 3 was maintained for 24 h with no detectable deactivation.

The dehydrogenation reaction was examined in the temperature range 723–773 K (He: $\text{H}_2$ : $\text{C}_3\text{H}_8 = 40:5:5$  ml/min) for both Ir + Sn/NaY and Ir-Sn/NaY. The activity data was similar for each system and is given in figure 4. Extrapolation of the data to 800 K, a point of known thermodynamic value [29], indicates that conversion of propane to propene (ca. 36%) was being performed near equilibrium levels (ca. 33%). The difference between the extrapolated and theoretical values is reasonable considering the errors present in controlling the reactant concentrations. That equilibrium levels of propene were being obtained was confirmed by the insignificant change in total propane conversion upon varying the amount of catalyst from 100 to 300 mg.

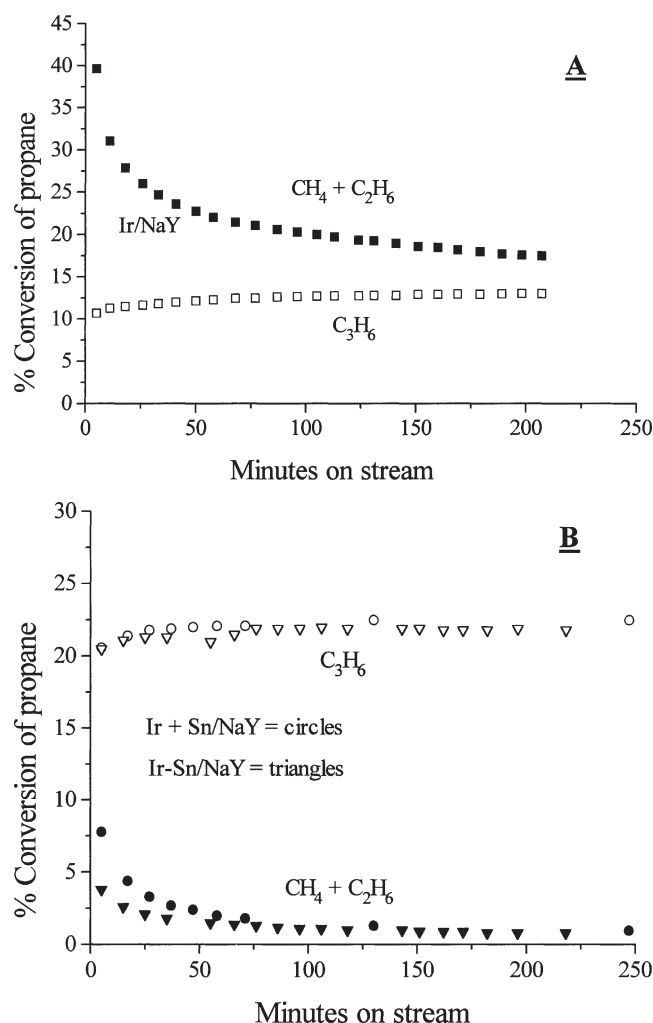


Figure 3. Propane dehydrogenation. Reaction conditions: 773 K,  $\text{He} : \text{H}_2 : \text{C}_3\text{H}_8 = 40 : 5 : 5$  ml/min. (A) (■) Ir/NaY, (B) (●) Ir + Sn/NaY, (▲) Ir-Sn/NaY.

**Temperature-programmed reaction (TPRE) of chemisorbed CO:** The TPRE profiles for Ir/NaY, Ir + Sn/NaY, and Ir-Sn/NaY are given in figure 5. The Ir/NaY catalyst desorbed CO to give three TPRE maxima at 392, 501 (sh), and 577 K. Methane was produced above 598 K with a maximum at 718 K and a low temperature shoulder at 658 K. The slow desorption of  $\text{H}_2\text{O}$  began at 648 K and continued at 773 K for 1–2 h. The TPRE profiles for Ir + Sn/NaY and Ir-Sn/NaY were essentially identical, with the desorption of CO displaying two maxima at 403 and 703 K. Neither  $\text{CH}_4$  nor  $\text{H}_2\text{O}$  was produced by the Ir/Sn catalysts. The TPRE profiles for the Ir and Ir/Sn catalysts were highly reproducible. Figure 6 shows repeated traces for the Ir + Sn/NaY catalyst.

#### 4. Discussion

Previous work has demonstrated that the use of  $\text{Ir}(\text{CO})_2(\text{acac})$  as a precursor allows the formation of highly dispersed Ir particles inside the pores of zeolite NaY and NaX [28,30–32]. It has also been shown that  $\text{SnMe}_4$  is

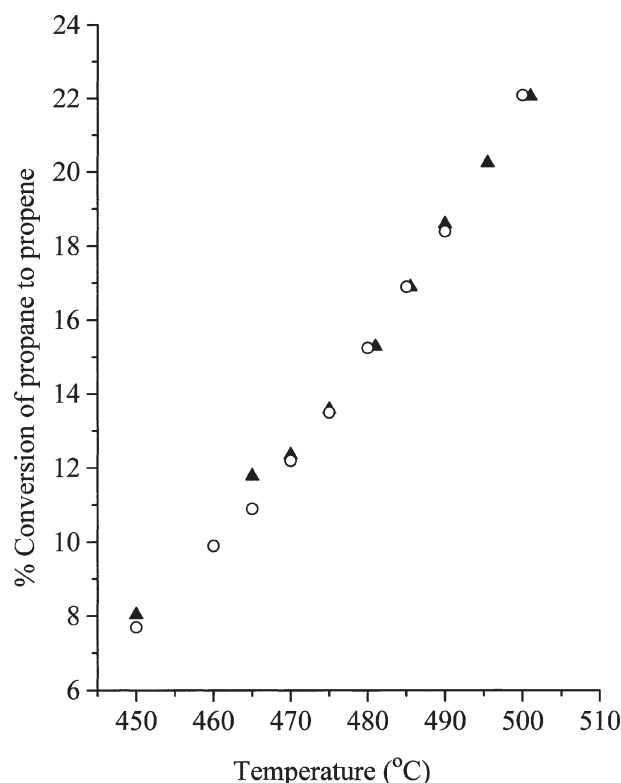


Figure 4. Propane dehydrogenation. Reaction conditions: 723–773 K,  $\text{He} : \text{H}_2 : \text{C}_3\text{H}_8 = 40 : 5 : 5$  ml/min. (○) Ir + Sn/NaY, (▲) Ir-Sn/NaY.

sufficiently small to enter zeolite NaY and form bimetallic particles with Pt [24]. Owing to the similar size of  $\text{SnMe}_3\text{OH}$  and  $\text{SnMe}_4$ ,  $\text{SnMe}_3\text{OH}$  should be able to enter the zeolite supercage with  $\text{Ir}(\text{CO})_2(\text{acac})$  and form bimetallic particles during activation in  $\text{H}_2$ . This proposition is consistent with our results that have shown the formation of highly dispersed bimetallic particles, when  $\text{Ir}(\text{CO})_2(\text{acac})$  and  $\text{SnMe}_3\text{OH}$  are used as catalyst precursors.

Interaction of a hexane solution of  $(\text{COD})_2\text{Ir-SnMe}_3$  with zeolite NaY resulted in the immediate adsorption of the organometallic complex as indicated by the solution becoming colorless and the zeolite becoming light red. The solid state structure of  $(\text{COD})_2\text{Ir-SnMe}_3$  indicates the molecule has trigonal bipyramidal coordination with the  $\text{SnMe}_3$  group in an equatorial position and each diene ligand spanning an axial and an equatorial site [25]. When the van der Waals radii of the protons on the cyclooctadiene ligands are included,  $(\text{COD})_2\text{Ir-SnMe}_3$  is calculated to have a molecular diameter of ca. 8.5 Å [25c]. The diameter of the precursor is therefore ca. 1.1 Å larger than the 7.4 Å openings of the zeolite supercage windows. Although fluxional processes within the molecule [25b] may make it possible for the precursor to enter the supercage with time, the immediate adsorption that occurred suggests the precursor was adsorbed onto the external zeolite surface. The change in color, from yellow to pink, which occurred upon adsorption, indicates that the precursor actually reacted with the zeolite surface and was not simply physisorbed. The presence of  $\text{C}_7/\text{C}_8$  species in the electron impact mass spec-

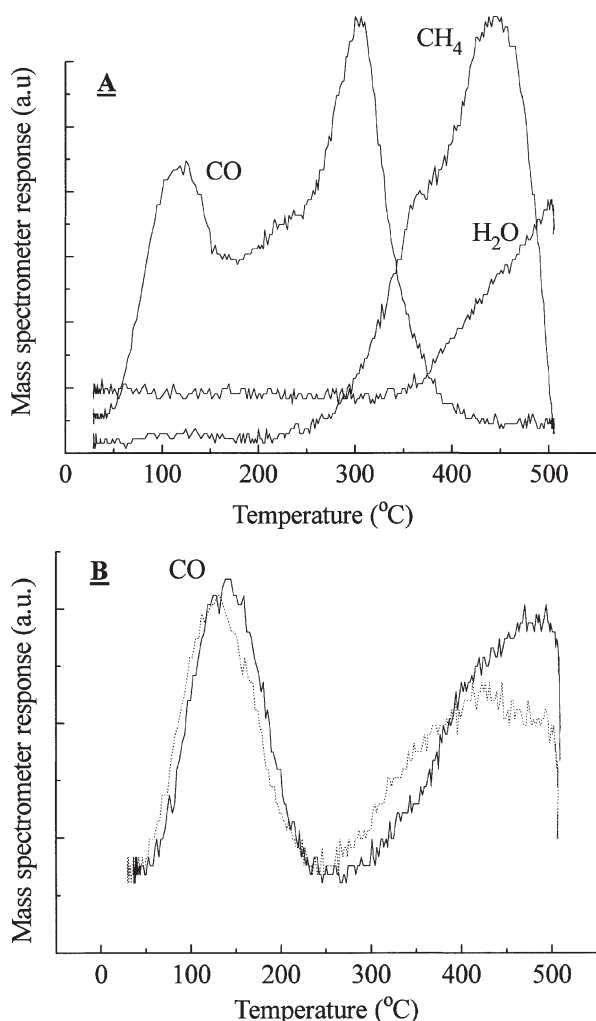


Figure 5. Temperature-programmed reaction of chemisorbed CO for (A) Ir/NaY, (B) Ir + Sn/NaY (solid line) and Ir-Sn/NaY (dashed line).

trum of the freshly prepared sample suggests that the precursor lost one or more cyclooctadiene ligands upon adsorption.

The strong interaction between  $(\text{COD})_2\text{Ir-SnMe}_3$  and NaY is in contrast to the results of other researchers who found that no chemical reaction occurred upon impregnating NaY with  $(\text{CO})_4\text{Co-SnMe}_3$  [33] or  $(\text{CO})_5\text{Mn-SnMe}_3$  [34]. One significant difference between our single-source precursor and these Co-Sn and Mn-Sn precursors is the presence of cyclooctadiene ligands instead of carbonyl ligands. The difference in reactivity could result from the relative lability of the CO versus the COD ligands.

Electron microscopy and visual inspection of our Ir/Sn/NaY materials revealed that metal particles of very different sizes were produced, depending upon whether single- or dual-source molecular precursors were used. The metal particles produced from the dual molecular precursors were found to be homogeneous in distribution and were in the 1 nm size range. In contrast, the metal particles produced from the single molecular precursor displayed a very broad (possibly bimodal) distribution with particles observed in both the nanometer and the millimeter size ranges.

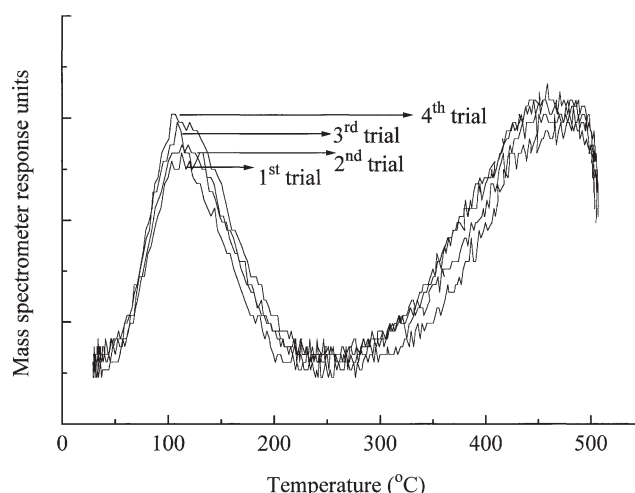


Figure 6. Sequential temperature-programmed reaction of chemisorbed CO for Ir + Sn/NaY.

Bein and coworkers observed the formation of nanoscale particles entrapped within zeolites NaY and MCM-41, when  $(\text{CO})_4\text{Co-SnMe}_3$  [33],  $(\text{CO})_5\text{Mn-SnMe}_3$  [34] and  $(\eta^5\text{-C}_5\text{H}_5)(\text{CO})_3\text{Mo-SnMe}_3$  [35] were activated under vacuum. This contrast to our result is probably ascribable to the location of the precursor during the activation process. It is expected that a precursor located in the supercages of NaY would be less mobile during activation than a precursor located on the external zeolite surface. The lower mobility should cause the precursors located in the supercages to produce much smaller particles than precursors located on the external zeolite surface, as observed.

The EDX analysis of the metal particles present in the two Ir/Sn/NaY systems showed that bimetallic particles were formed in each case. Although some areas of the catalysts contained Sn but not Ir, no particles were found that contained Ir only. The primary difference between the Ir-Sn/NaY and Ir + Sn/NaY samples was that the larger particles present in Ir-Sn/NaY were ca. 1:1 Ir:Sn alloys, while the smaller particles present in Ir + Sn/NaY were slightly Ir-rich. The EDX results were consistent with the methods of catalyst preparation employed. It is expected that delivering Ir and Sn to the support in a single complex will promote the formation of bimetallic particles that have an atomic composition close to that of the precursor. In the case of dual molecular precursors, it is more difficult to control the formation of bimetallic particles and to prevent a significant portion of the Sn from interacting strongly with the support.

Comparison of the hydrogenolysis/dehydrogenation properties of the Ir/Sn/NaY catalysts with a homometallic Ir/NaY catalyst showed that the two systems were remarkably different. As depicted in figure 1, the presence of Sn dramatically diminished the capacity for both primary (propane to methane and ethane) and secondary (ethane to methane) hydrogenolysis reactions. The hydrogenolysis of an alkane is a structure-sensitive reaction, requiring ca. 12 metal atoms for the active site [36–39]. In addition

to structure sensitivity, the hydrogenolysis reaction is affected by the electronic nature of the active metal particles. Electron-rich metals are commonly much less active for carbon-carbon bond cleavage than electron-deficient metals. This trend is demonstrated in the relative activity of different metals for the hydrogenolysis of ethane, which is generally taken to be:  $\text{Ru} > \text{Rh} > \text{Ir} > \text{Pt-Pd}$  [40]. As the Ir+Sn/NaY catalyst contained metal particles that were similar in size to those present in the Ir/NaY catalyst [28], the decreased hydrogenolysis activity of Ir+Sn/NaY cannot be explained by dispersion effects. However, the relatively low hydrogenolysis activity of the Ir/Sn/NaY catalysts could be due to dilution of catalytically active Ir ensembles with inactive Sn atoms and/or the formation of electronically rich Ir ensembles through alloying with Sn.

Carbon monoxide adsorption and reaction has been used to probe the nature of the three catalyst materials (see figure 5). The temperature-programmed reaction (TPRE) of chemisorbed CO was very similar for both Ir+Sn/NaY and Ir-Sn/NaY. Both catalysts desorbed CO over the same temperature range, and there was no evidence for formation of  $\text{CH}_4$ . The CO desorption profiles were highly reproducible, as shown in figure 6, implying no sequential buildup of surface species. In contrast, the TPRE profile for Ir/NaY showed a low-temperature desorption of CO followed at higher temperature by desorption of  $\text{CH}_4$  and  $\text{H}_2\text{O}$ . The latter products result from the hydrogenation of surface carbide and oxide species generated by the cleavage of CO. The TPRE profile obtained for the Ir/NaY catalyst was similar to results obtained for other supported Ir catalysts [41].

The cleavage of CO apparently does not require as many contiguous metal atoms (ca. 4–5 metal atoms) [36], as does the hydrogenolysis of propane (ca. 12 atoms) [36–39], yet the Ir/Sn/NaY catalysts do display activity for the hydrogenolysis reaction. The absence of CO cleavage is, therefore, unlikely to be the result of ensemble size-limiting effects but rather the probable result of electronic modification of Ir to produce a particle surface that is incapable of breaking the CO bond. Although the detailed morphology of the Ir/Sn nanoparticles could be different under hydrogenolysis conditions ( $\text{H}_2$  vs. CO atmosphere, higher temperature) [42], it, nevertheless, is likely that Sn acts as a “ligand” to modify the hydrogenolysis activity of the Ir ensembles and not solely as an inert diluent. This conclusion contrasts with results on the related Pt/Sn/NaY [24] and Pt/In/NaY [43] systems by Mériaudeau and coworkers, who have attributed the diminished hydrogenolysis activity displayed by these catalysts to ensemble dilution effects alone.

A portion of the difference in hydrogenolysis activities observed for the Ir+Sn/NaY and Ir-Sn/NaY catalysts may also be due to electronic differences between the two systems, since the EDX results suggested a net higher (closer to 1:1) Sn:Ir ratio for the less active Ir-Sn/NaY material. However, it is difficult to separate this effect from the effect of the gross structural differences between the two

systems. Since the dispersion of the Ir-Sn/NaY catalyst is significantly lower than that of Ir+Sn/NaY catalyst, the decreased hydrogenolysis activity of Ir-Sn/NaY can also be attributed to the reduced number of active sites that necessarily accompanies a low metal dispersion. Related evidence can be drawn also from the dehydrogenation of propene performed in the absence of  $\text{H}_2$ . Although propane dehydrogenation is a structure-insensitive reaction [44], if equilibrium conversions are not being obtained, then the rate will depend upon the number of active sites present. The higher initial activity and slower rate of deactivation of Ir+Sn/NaY, in comparison to Ir-Sn/NaY, are consistent with the presence of more active sites in Ir+Sn/NaY.

## 5. Conclusions

The preparation of zeolite-NaY-supported Ir/Sn catalysts has been examined through the use of single-source and dual-source organometallic precursors. Energy-dispersive X-ray analysis established that bimetallic particles were formed in each case. The catalyst prepared from the dual precursor source contained a homogeneous distribution of metal particles ca. 1 nm in size. The catalyst prepared from the single-source precursor contained a heterogeneous distribution of metal particles, with particles in both the nanometer and millimeter size ranges.

The Ir/Sn/NaY catalysts were examined for the dehydrogenation of propane, propane hydrogenolysis, and the temperature-programmed reaction of CO. Both Ir/Sn/NaY catalysts dehydrogenated propane to propene with >95% selectivity at 773 K (ca. 20% conversion) and exhibited very good stability with time on stream. Both Ir/Sn/NaY catalysts also desorbed CO in a similar temperature range and without the production of  $\text{CH}_4$ . Comparison with an Ir/NaY catalyst suggested that the catalytic activity of the Ir/Sn/NaY system was determined by electronic modification of Ir by Sn as well as by dilution of active Ir ensembles.

## Acknowledgement

This research was supported in part by the National Science Foundation, grant No. DMR 89-20538 to the Seitz Materials Research Laboratory at the University of Illinois. Electron microscopy and EDX experiments were performed at the Center for Microanalysis of Materials, University of Illinois, which is supported by the US Department of Energy under grant DEFG02-91-ER45439. Electron impact mass spectra were provided by the staff of the Mass Spectrometry Laboratory, School of Chemical Sciences, University of Illinois. The authors appreciate the donation of NaY by Dr. W. Wachter from Exxon Research and Development Laboratory. Mr. Dan Hay is acknowledged for his preparation of  $(\text{COD})_2\text{Ir-SnMe}_3$ .

## References

- [1] C.N. Satterfield, *Heterogeneous Catalysis in Industrial Practice*, 2nd Ed. (McGraw-Hill, New York, 1991).
- [2] J.H. Sinfelt, *Bimetallic Catalysts – Discoveries, Concepts, and Applications* (Wiley, New York, 1983).
- [3] (a) D. Nazimek, *React. Kinet. Catal. Lett.* 13 (1980) 155;  
(b) G.C. Bond and X. Yide, *J. Mol. Catal.* 25 (1984) 141;  
(c) M. Sprock, X. Wu and T.S. King, *J. Catal.* 138 (1992) 617;  
(d) T.J. Plunkett and J.K.A. Clarke, *J. Catal.* 35 (1974) 330;  
(e) K. Foger and J.R. Anderson, *J. Catal.* 64 (1980) 448.
- [4] L. Guzzi and A. Sárkány, in: *Catalysis*, Vol. 11 (Royal Society of Chemistry, Cambridge, 1994) p. 319 and references therein.
- [5] J. Llorca, N. Homs, J.-L.G. Fierro and P. Ramirez de la Piscina, *J. Catal.* 166 (1997) 44.
- [6] R.D. Cortright and J.A. Dumesic, *J. Catal.* 157 (1995) 576.
- [7] E. Merlen, P. Beccat, J.C. Bertolini, P. Delichère, N. Zanier and B. Didillon, *J. Catal.* 159 (1996) 178.
- [8] F.B. Passos, M. Schmal and M.A. Vannice, *J. Catal.* 160 (1996) 118.
- [9] B. Shi and B.H. Davis, *J. Catal.* 157 (1995) 626.
- [10] F. Coloma, A. Sepúlveda-Escribano, J.-L.G. Fierro and F. Rodríguez-Reinoso, *Appl. Catal.* 148 (1996) 63.
- [11] O.D. Bariäs, A. Holmen and E.A. Blekkan, *J. Catal.* 158 (1995) 1.
- [12] S.M. Stagg, C.A. Querini, W.E. Alvarez and D.E. Resasco, *J. Catal.* 168 (1997) 75.
- [13] J. Llorca, P.R. Delapiscina, J.-L.G. Fierro, J. Sales and N. Homs, *J. Mol. Catal. A* 118 (1997) 1381.
- [14] C. Yokoyama, S.S. Bhargadwaj and L.D. Schmidt, *Catal. Lett.* 38 (1996) 181.
- [15] US Patent 4,966,880 to Exxon Research and Engineering Corporation (1990).
- [16] US Patent 5,609,751 to Chevron Chemical Company (1997).
- [17] US Patent 5,516,741 to Johnson Matthey Public Limited Company (1996).
- [18] US Patent 4,786,625 to UOP Inc. (1988).
- [19] US Patent 5,221,465 to Exxon Research and Engineering Corporation (1993).
- [20] US Patent 5,122,489 to Mobil Oil Corporation (1992).
- [21] US Patent 5,413,976 to Mazda Motor Corporation (1995).
- [22] R. Fréty, B. Benaichouba, P. Bussière, D.S. Cunha and Y.L. Lam, *J. Mol. Catal.* 25 (1984) 173.
- [23] K. Lázár, P. Bussière, M. Guénin and R. Fréty, *Appl. Catal.* 38 (1988) 19.
- [24] (a) P. Mériaudeau, C. Naccache, A. Thangaraj, C.L. Bianchi, R. Carli, V. Vishvanathan and S. Narayanan, *J. Catal.* 154 (1995) 345;  
(b) P. Mériaudeau, A. Thangaraj, J.F. Dutel and C. Naccache, *J. Catal.* 167 (1997) 180.
- [25] (a) J.R. Shapley, Ph.D. thesis, Harvard University (1972);  
(b) J.R. Shapley and J.A. Osborn, *Acc. Chem. Res.* 6 (1973) 305;  
(c) D.N.T. Hay and J.R. Shapley, unpublished results.
- [26] D. Roberto, E. Cariati, R. Psaro and R. Ugo, *Organometallics* 13 (1994) 4227.
- [27] (a) M.A. Urbancic, Ph.D. thesis, University of Illinois at Urbana-Champaign (1984);  
(b) P.D. Lane, Ph.D. thesis, University of Illinois at Urbana-Champaign (1995).
- [28] D.M. Somerville, M.S. Nashner, R.G. Nuzzo and J.R. Shapley, *Catal. Lett.* 47 (1997) 17.
- [29] *Selected Values of Properties of Hydrocarbons and Related Compounds* (Chemical and Petroleum Research Laboratory, Carnegie Institute of Technology, Pittsburgh, 1958).
- [30] S. Kawi, J.-R. Chang and B.C. Gates, *J. Am. Chem. Soc.* 115 (1993) 4830.
- [31] S. Kawi and B.C. Gates, *J. Phys. Chem.* 99 (1995) 8824.
- [32] S. Kawi, J.-R. Chang and B.C. Gates, *J. Catal.* 142 (1993) 585.
- [33] C. Huber, K. Moller and T. Bein, *J. Phys. Chem.* 98 (1994) 12067.
- [34] A. Borvornwattananont and T. Bein, *J. Phys. Chem.* 96 (1992) 9447.
- [35] C. Huber, K. Moller and T. Bein, *J. Chem. Soc. Chem. Commun.* (1994) 2619.
- [36] G.A. Martin, *Cat. Rev. Sci. Eng.* 30 (1988) 519.
- [37] J.A. Dalmon and G.A. Martin, *J. Catal.* 66 (1980) 214.
- [38] Y.H. Romdhane, B. Bellamy, A. de Gouveia and M. Che, *Appl. Surf. Sci.* 31 (1988) 55.
- [39] B. Chen and J.G. Goodwin, Jr., *J. Catal.* 158 (1996) 228.
- [40] J.H. Sinfelt, *Catal. Rev. Sci. Eng.* 3 (1969) 175.
- [41] J.R. Shapley, W.S. Uchiyama and R.A. Scott, *J. Phys. Chem.* 94 (1990) 1190.
- [42] M.S. Nashner, D.M. Somerville, P.D. Lane, D.L. Adler, J.R. Shapley and R.G. Nuzzo, *J. Am. Chem. Soc.* 118 (1996) 12964.
- [43] (a) P. Mériaudeau, C. Naccache, A. Thangaraj, C.L. Bianchi, R. Carli and S. Narayanan, *J. Catal.* 152 (1995) 313;  
(b) P. Mériaudeau, A. Auroux and C. Viornery, *Catal. Lett.* 41 (1996) 139;  
(c) P. Mériaudeau, A. Thangaraj, J.F. Dutel, P. Gelin and C. Naccache, *J. Catal.* 163 (1996) 338.
- [44] D.E. Resasco and G.L. Haller, in: *Catalysis*, Vol. 11 (Royal Society of Chemistry, Cambridge, 1994) p. 379.